

Electronic, magnetic, and structural properties of $L1_0\text{FePt}_x\text{Pd}_{1-x}$ alloys

S. D. Willoughby and J. M. MacLaren

Physics Department, Tulane University, New Orleans, Louisiana 70118

T. Ohkubo, Sangki Jeong, Michael McHenry, and David E. Laughlin

Materials Science and Engineering Department, Data Storage Systems Center, Carnegie Mellon University, Pittsburgh, Pennsylvania 15213

Sang-Jun Choi and Soon-Ju Kwon

Department of Material Science and Engineering, Postech Pohang, 790-784 South Korea

We present theoretical and experimental results on the electronic, magnetic, and structural properties of $L1_0$ FePd, FePt, and $\text{FePt}_x\text{Pd}_{1-x}$ alloys. These alloys have large magnetizations and magnetocrystalline anisotropies and as such are potentially technologically important for applications as permanent magnets or high-density storage media. Results of first principles electronic structure calculations show that the system is a strong ferromagnet with an almost full majority Fe band, and that magnetization and magnetocrystalline anisotropy remain large over the range of composition. Total energy calculations predict phase separation on the disordered Pd/Pt layer at low temperatures. Experimental studies using energy dispersion x-ray line scans confirm regions that are Pt rich and Pd rich forming at low temperatures. © 2002 American Institute of Physics. [DOI: 10.1063/1.1450850]

I. INTRODUCTION

Compounds that form in the $L1_0$ crystal structure have potential applications in permanent magnets and high density data storage since the structure produces useful magnetic properties as a direct result of a natural [001] superlattice. This paper will consider $L1_0$ alloys of the form $\text{FePt}_x\text{Pd}_{1-x}$ that have disordered Pt–Pd planes sandwiched between ordered Fe planes stacked along the [001] direction. These $L1_0$ alloys have large magnetizations, resulting from the two dimensional Fe layer, and large magnetocrystalline anisotropies because of the natural layering in the crystal.

The layer Korringa–Kohn–Rostoker method (LKKR) was used for all of the electronic structure calculations.¹ The disordered layer is dealt with via the coherent potential approximation (CPA), which has been successfully used in the past to calculate properties of disordered magnetic alloys.² Using the CPA in the LKKR method allows the calculation of the disordered $\text{FePt}_x\text{Pd}_{1-x}$ alloys within the same set of approximations as both ordered FePt and FePd. Using this *ab initio* approach we have calculated the magnetization, electronic structure, anisotropy, and enthalpy of mixing for the whole range of alloys from FePd to FePt.

We have explored partitioning of Pt and Pd in alternate [100] planes for ternary $\text{FePt}_x\text{Pd}_{1-x}$ materials. These $L1_0$ alloys are made by quenching from the high temperature disordered cubic phase. The kinetic driving force is dependent upon the transformation temperature. One possibility is that the alloys containing Pd/Pt may have several low temperature $L1_0$ phases, one with a disordered Pt/Pd layer, and others with phase separated FePt and FePd. Our hypothesis was that maybe these $L1_0$ alloys may be easier to make experimentally than either FePt or FePd. While we have not studied the full cubic to tetragonal order–disorder transition, it is still of interest scientifically to study the ordering in the Pt/Pd layer. Work is in progress on the studies of the cubic to

tetragonal transformation. Our total energy calculations show that Pd and Pt obey a pseudobinary phase diagram, suggesting phase separation at low temperatures. Sample alloys were prepared by arc melting, then characterized by EDX and studied by XRD and TEM.

II. THEORETICAL RESULTS

Lattice constants for FePt (an a of 4.00 Å, and c/a of 0.918) and FePd (an a of 3.855 Å, and c/a of 0.963) were taken from Pearson's.³ These are close to the values obtained from our density functional theory calculations using the Vienna *ab-initio* simulation package.⁴ The values for a and c/a for the disordered alloys were linearly interpolated between the values of the two pure alloys. As a direct result of the structure, density of states calculations of the alloys show that the majority Fe band is nearly full, leading to strong ferromagnetism. The Fermi energy passes through a local minimum in the minority band, providing a rationale for the stability of the structure. Unlike the density of states of many alloys, the sharp structure of the ordered compounds is preserved, reflecting the electronic similarity between Pt and Pd, consistent with the ease of formation of these alloys.

The calculated magnetization varies somewhat slowly through the entire series, with a value of 1050 emu/cm³ for FePd and 1070 emu/cm³ for FePt. As expected the magnetism is dominated by the Fe moment. As the series crosses from FePd to FePt the a lattice constant increases slightly, and the c/a ratio is reduced. A larger separation of the Fe atoms gives rise to a small increase in local moment as seen in the calculations.

The magnetocrystalline anisotropy as a function of composition is shown in Fig. 1. The calculations were performed using the force theorem⁵ with spin–orbit coupling included. The magnetocrystalline anisotropy was determined based on the difference in band energies between the hard axis and

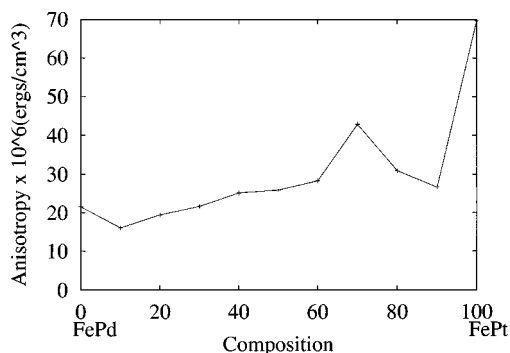


FIG. 1. Magnetocrystalline anisotropy for $\text{FePt}_x\text{Pd}_{1-x}$ ($\text{Fe}_{1-x}\text{Co}_x\text{Pt}$).

easy axis of magnetization. The anisotropy does not remain constant throughout the series; there is a peak around $\text{FePt}_{70}\text{Pd}_{30}$. The experimental anisotropy of pure FePt is 66×10^6 ergs/cm³ (Ref. 6) while the anisotropy of FePd is 6.6×10^6 ergs/cm³.⁷ These can be compared to the calculated values of 70×10^6 ergs/cm³ and 21×10^6 ergs/cm³, respectively. The overall trend is a decrease in the anisotropy with increasing Pd content as might be expected simply from the strength of the spin-orbit coupling. Though the a lattice constant decreases, the c/a ratio increases in going from FePt to FePd , causing the layers to spread apart. These materials have a large magnetostriction, so the anisotropy is expected to be sensitive to the lattice constants. The anisotropy of pure FePt rises nearly linearly as the lattice constant is contracted and c/a expanded. The composition dependence of the anisotropy reflects the competing effects of structure and spin-orbit coupling.

We now discuss the possibility of phase separation in the disordered Pd/Pt layer. The free energy is constructed from the total energy calculated for the alloys and ordered compounds, and a simple entropy of mixing term. Using a common tangent construction, one can form a pseudobinary phase diagram. We predict phase separation below 650 °C, at which point the Pt-Pd layer will separate into Pt rich and Pd rich regions. Figure 2 shows the change in enthalpy of mixing versus composition for $\text{FePt}_x\text{Pd}_{1-x}$ as well as for $\text{Fe}_{1-x}\text{Co}_x\text{Pt}$. As can be seen, the positive energy of mixing suggests phase separation at low temperatures for both the

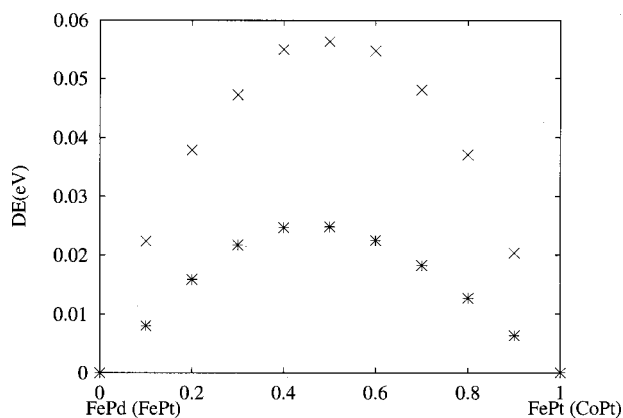


FIG. 2. Energy difference versus composition for $\text{FePt}_x\text{Pd}_{1-x}$ (x) and $\text{Fe}_{1-x}\text{Co}_x\text{Pt}$ (*).

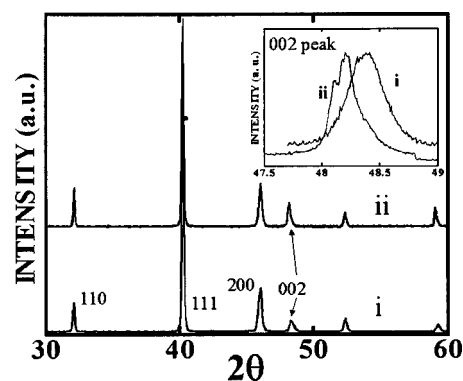


FIG. 3. Synchrotron XRD patterns for FePdPt after annealing treatment; the inset shows the (002) peaks with the slow scan rates. Specimens are annealed at (i) 500 °C for 120 hours and annealed at (ii) 700 °C for 60 hours after homogenization. Specimens are water quenched from homogenization temperature.

$\text{FePt}_x\text{Pd}_{1-x}$ and $\text{Fe}_{1-x}\text{Co}_x\text{Pt}$ (Ref. 8) alloys. The driving force for phase separation is greater in $\text{FePt}_x\text{Pd}_{1-x}$ than $\text{Fe}_{1-x}\text{Co}_x\text{Pt}$ as indicated by the greater energies of mixing. The larger energy of mixing seen in the $\text{FePt}_x\text{Pd}_{1-x}$ system is attributed to the greater difference in size between Pt and Pd. Substituting Co for Fe is energetically easier than substituting Pt for Pd.

III. EXPERIMENTAL RESULTS AND DISCUSSION

To compliment our theoretical work we have also studied these alloys experimentally. Alloys of $\text{Fe}_{50}\text{Pt}_{25}\text{Pd}_{25}$ were prepared in an argon atmosphere from high purity starting materials using an arc-melting method. The chemical composition of the alloy was determined to be $\text{Fe}_{49}\text{Pt}_{25}\text{Pd}_{26}$ by energy dispersive x-ray (EDX) analysis. The initial process of the as-cast alloy involved annealing for homogenization at 1400 °C for 5 hours. The samples were water quenched from the homogenization temperature. The as-quenched materials were disordered, showing fcc phase in XRD patterns. These materials were subsequently annealed at 500 °C for 120 hours and 700 °C for 60 hours to obtain the $L1_0$ tetragonal ordered structure, removing all the fcc phase.

XRD spectra using Synchrotron radiation (Postech) confirmed the full ordering, showing the clear splitting of 002 and 200 reflections without any remaining fcc phase as seen in Fig. 3. These experiments use mainly Ni K edge as a radiation source which has a wavelength of 1.151 196 Å. The inset in Fig. 3 shows x-ray spectrum around the nominal 002 peak determined with a slow scan rate. This peak indicates the possibility of phase separation as evident from the peak splitting as well as peak broadening due to the overlapping of several 002 reflections. However, this broadening makes it difficult to identify the individual peaks. Indeed, FePd and FePt have similar lattice parameters. Therefore, the angular difference 2θ (θ : Bragg angle of 002 peak) between 002 peaks in each is $\sim 0.1^\circ$. The specimen annealed at 500 °C shows a large amount of peak broadening, implying overlapping of several peaks. Further x-ray data taken using the longer wavelength Cr radiation source shows similar results. The shift in the 002 peak at these two different annealing

temperatures cannot be quantitatively determined. However, it can be attributed to the higher degree of order in the 500 °C (smaller lattice parameter of c axes direction), assuming these alloys are in equilibrium states.

Detailed TEM analysis was performed to investigate the possibility of phase separation and determination of where the chemical segregation occurs. Theoretically, the phase separation of the $L1_0$ phase lowers the free energy in the ternary $L1_0$ system as discussed in the preceding section (though the electronic structure calculations only rigorously predict a two dimensional miscibility). EDX studies were carried out using scanning transmission microscopy using a Philips Technai STEM Polytwinned structure which has a hierarchy of microtwins⁹ that can be observed by TEM analysis.

Three structural variants are observed in selected area diffraction (SAD) patterns. In the inside of a single structural variant, a fine fringe with the length scale of ~ 6 nm was observed in the bright field image. To exclude the possibility of Moire fringe contrast by overlapping with another structural variant, we have chosen only one structural variant region [as confirmed by SAD patterns at high magnification, as seen in Fig. 4(a) and 4(b)]. On the $[101]$ zone axes of the SAD patterns diffuse satellites are observed around each main reflection close to the $[101]$ direction. Spatially resolved chemical analysis is difficult on this small length scale, especially with small differences in compositions. However, there is evidence for phase separation in the $L1_0$ phase, though the amount of chemical segregation is difficult to determine. Fluctuations in the Pd and Pt concentrations can be observed in Fig. 4(c) by means of EDX (STEM mode) line scans of 50 nm across the modulated fringe region. Two distinct regions can be observed from this analysis. One is a Pd enriched region and the other is a Pt enriched region. This feature is evidence for the decomposition possibly from an unstable ternary $L1_0$ to two stable $L1_0$ phases which are approaching their respective binary compositions that form as a result of chemical modulation.

IV. CONCLUSIONS

In this article we have studied magnetic and structural properties of $L1_0$ $\text{FePt}_x\text{Pd}_{1-x}$ series. We have found strong ferromagnetism in all of the alloys considered, with a nearly full majority Fe band. The magnetization, which varies slowly throughout the whole series, is determined by the Fe local moment. The anisotropy calculations show a maximum around $\text{FePt}_{70}\text{Pd}_{30}$, reflecting a competition between the composition dependence of the lattice constant (and its strong effect on the anisotropy) and the strength of spin-orbit coupling. Total energy calculations have been used to construct a pseudobinary phase diagram for $\text{FePt}_x\text{Pd}_{1-x}$, which follows a regular solution model. We predict phase separation into Pt and Pd rich phases below 650 °C. Experimental observations show regions of phase separation at low

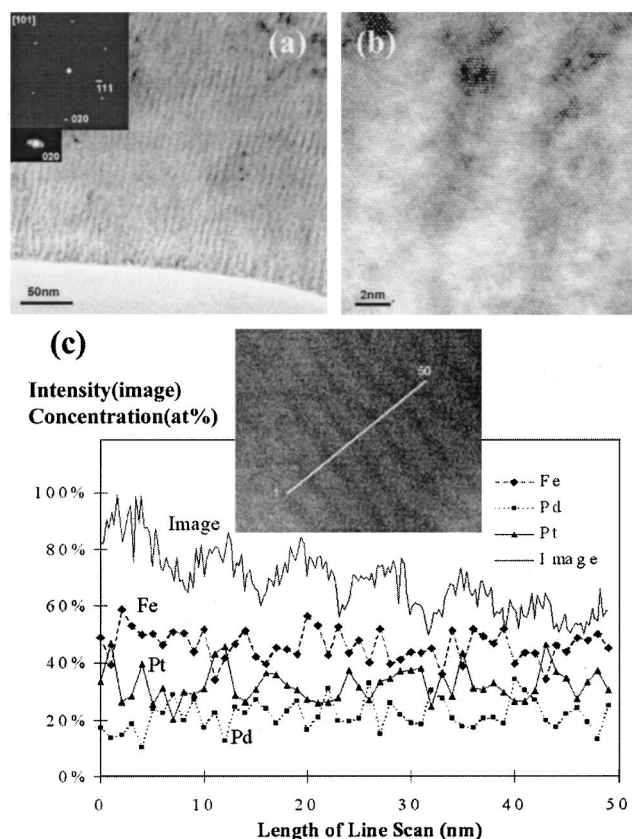


FIG. 4. (a) Bright field image, SAD patterns, as well as (b) HRTEM image for the specimens annealed at 700 °C for 120 hours. With the same specimen, (c) shows a chemical analysis with the line scan method. EDX (STEM) was used for analysis method.

temperature, though we cannot resolve if they occur directly from the disordered cubic alloy, or from the in-plane ordering in disordered $L1_0$ $\text{FePt}_x\text{Pd}_{1-x}$.

ACKNOWLEDGMENTS

The authors gratefully acknowledge the support of the National Science Foundation, Award No. DMR-9971573, and DARPA Award MDA 972-97-1-003. The CMU authors gratefully acknowledge the support of the National Science Foundation, Award No. ECD-89-07068.

¹J. MacLaren, D. Vvdsensky, R. Albers, and J. Pendry, *Comput. Phys. Commun.* **60**, 365 (1990).

²J. MacLaren and R. Victora, *J. Appl. Phys.* **76**, 6069 (1994).

³*Pearson's Handbook for Crystallographic Data*, edited by P. Villars (ASM International, Materials Park, OH, 1997), Vol. 2.

⁴J. F. G. Kresse, Vienna ab-initio simulation package, 2001.

⁵A. Makintosh and O. Anderson, *Electrons at the Fermi Surface* (Cambridge University Press, London, 1980).

⁶J. Liu, C. Lou, Y. Liu, and D. Sellmyer, *Appl. Phys. Lett.* **72**, 483 (1998).

⁷C. Bourgonon, S. Takarenko, J. Cibert, B. Gilles, A. Marty, and Y. Sampson, *Appl. Phys. Lett.* **75**, 2818 (1999).

⁸J. MacLaren, S. Willoughby, M. McHenry, B. Ramalingam, and S. G. Sankar, *IEEE Trans. Magn.* **37**, 1272 (2001).

⁹B. Zhang, Ph.D. thesis, University of Pittsburgh, 1991.